EUROGRAPHICS Workshop on Graphics and Cultural Heritage (2018)
R. Sablatnig and M. Wimmer (Editors)

Aging Prediction of Cultural Heritage Samples Based on Surface Microgeometry

I. M. Ciortan[1], G. Marchioro[1], C. Daffara[1], R. Pintus[2], E. Gobbetti[2] and A. Giachetti[1]

[1]Computer Science Department, University of Verona, Italy
[2]Visual Computing Group, Center for Advanced Studies, Research and Development in Sardinia, Italy

Abstract

A critical and challenging aspect for the study of Cultural Heritage (CH) assets is related to the characterization of the materials that compose them and to the variation of these materials with time. In this paper, we exploit a realistic dataset of artificially aged metallic samples treated with different coatings commonly used for artworks' protection in order to evaluate different approaches to extract material features from high-resolution depth maps. In particular, we estimated, on microprofilometric surface acquisitions of the samples, performed at different aging steps, standard roughness descriptors used in materials science as well as classical and recent image texture descriptors. We analyzed the ability of the features to discriminate different aging steps and performed supervised classification tests showing the feasibility of a texture-based aging analysis and the effectiveness of coatings in reducing the surfaces' change with time.

CCS Concepts

•***Computing methodologies*** → ***Machine learning approaches;*** *Neural networks;* •***Applied computing*** → ***Arts and humanities;*** •***General and reference*** → *Metrics;*

1. Introduction

An important visual computing task related to Cultural Heritage (CH) objects' study and conservation is the characterization of surfaces at microscopic level and the analysis of how their shapes change over time.

Microprofilometric probes [SB00] can reconstruct surfaces with a micrometric resolution, and the characteristics of the measured surface patterns can give important information about the physical, chemical properties and appearance of the material. Surface metrology provides well established tools to quantitatively analyze roughness patterns, by using methodologies and parameters described in ISO standards related to profile analysis and areal characterization [Bla13].

These measurements have been seldom evaluated in comparative works with the purpose of classifying specific materials of interest. This task, however, is particularly interesting in the CH domain, where the analysis of material properties and their evolution due to both time and different environmental conditions is particularly useful for conservators.

The problem is non-trivial as many factors influence the texture pattern of the surface depth at different scales.

In this paper, we present results of tests aimed at using surface metrology tools as well as different image processing techniques to characterize and classify, according to aging, samples of bronze and silver alloys typically used in artworks.

Our testbed consists of Cultural Heritage material samples artificially aged provided by an Italian art conservation and restoration laboratory.

2. Related Work

Several descriptors are already used in material science to characterize surface roughness. Profile parameters are usually exploited in material science to characterize roughness from linear measurements. To deal with surface capture, aerial parameters are described in the ISO25178 standard to characterize materials [Bla13] or to analyze the relevance of parameters during surface-changing processes [DKB14, VGBEM*10].

In the image processing domain, there are many other methods commonly used to characterize statistical properties of a signal regularly sampled in 2D, i.e. the texture pattern [TJ*93]. In principle, all those descriptors can be applied as well for depth map description. A survey of specific issues of texture analysis methods for material science is presented in [Bun13]. Examples of different texture characterization methods not included in surface metrology protocols are second order statistics like co-occurrence matrices [Har79] describing joint variations of gray-scale at selected distances. Local binary patterns [GZZ10] are other popular visual descriptors measuring robust statistics of pixel neighborhoods. Another classical

DOI: 10.2312/gch.20181352

texture analysis method, not included in surface roughness analysis protocols is the characterization of patch properties using statistics of filter banks' output [VZ02].

Recent advances in texture analysis revealed that other methods based on learned representations of local patterns can outperform the classical ones for classification, using joint distribution of neighboring pixels [VZ03], advanced key-point descriptors like SIFT coupled with encoders like Fisher Vectors, or feature extraction methods based on Convolutional Neural Networks (CNN) training [CMK*14, CMKV16].

Feature extraction refers to using a pre-trained deep neural network and activate it in order to compute features for a new dataset at a certain layer in the architecture of the network. The choice of the activation layer is mainly a choice of design preference, even though there is a certain dependency between the similarity of the target data and the data that was used to train the pre-trained network: the more they are similar, deeper layers in the architecture can be chosen. This is mainly due to the fact that early layers learn low-level features (edges, blobs, color), while last layers learn task-specific, high-level features. Two notable works that implemented the reuse of pretrained CNNs for texture analysis are presented in [CMK*14] and [CMKV16]. In the former one, they load the AlexNet model, while in latter they use the VGG models. The AlexNet network (8 layer architecture) was trained on a subset of the ImageNet database (more than a million images) for the Large-Scale Visual Recognition Challenge [RDS*15] (ILSVRC 2012) and can classify images into 1000 object categories. Hence, the model has learned rich feature representations for a wide range of images. Meanwhile, the VGG models have won the ILSVRC 2014 and are designed according to a deeper architecture (16 and 19 layers).

To our knowledge, there is no previous work in the literature that tested both ISO descriptors and texture analysis methods together and compared their ability to discriminate the roughness of different materials employed in CH objects.

It would be therefore extremely useful to understand how specific standard parameters and texture analysis methods can be useful for this specific task.

For this reason we performed a study aimed at the evaluation of different roughness characterization methods on artificially aged metallic objects.

3. Study design

This research features metallic samples artificially degraded in an aging chamber. The samples were created by a conservation laboratory involved in a vast research project aimed at the characterization of artworks. The samples are made of silver alloys and bronze alloys. Each dataset has a reference plate left uncoated and the rest treated with distinct coatings (one different coating per plate) typically used in CH to prevent or at least slow down the aging process. The appearance of the uncoated samples between the different aging steps is shown in Figure 1. It is possible to see that evident changes appear in the material at a macroscopic level, however we are interested in using the microsurface analysis to find if some consistent changes in the surface depth properties can be measured with time evolution.

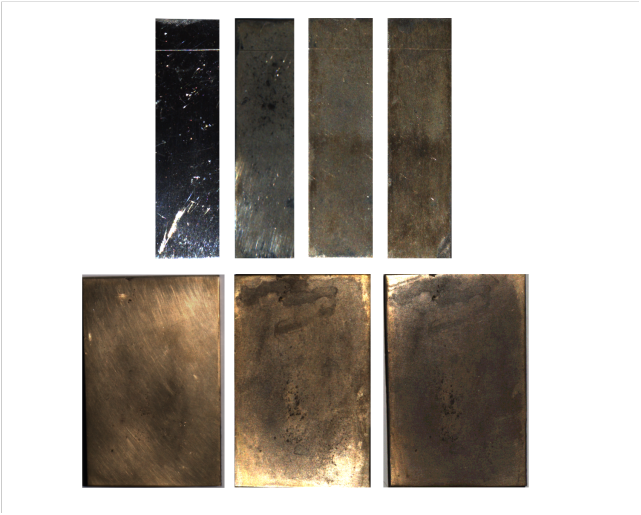

Figure 1: *The uncoated silver sample (top) at aging steps t_0, t_1, t_2, t_3 and the uncoated bronze sample (bottom) at t_0, t_1, t_2.*

The silver plates have the dimensions of approximately 7×2.5 cm, with a thickness of 0.1 cm, and they were cut from a sheet of sterling silver (alloy of silver 92.5% and copper 7.5%), undergoing additional polishing and brushing steps. The coatings that have been applied to the silver plates for preventing the fast aging effects are those widely used by the conservator's community and are based on acrylic resin and wax.

The bronze samples were created as an alloy of 90% copper and 10% tin, because this is the most representative mix employed in arts, dating as far as the ancient times and common as well for the Renaissance period. Each bronze coupon has a dimension of 8×5 cm and a thickness of 0.4 cm. The coatings applied to the bronze samples, as simple, blended or layered combinations, are those most encountered in the conservation community: acrylic resin (incral44) and soter wax. The coating should protect against corrosion that is the principal aging danger to which the bronze alloys kept in outdoor environments are susceptible to. Considering this, the artificial aging of the bronzes was performed by simulating the outdoor conditions in a test chamber. Surface acquisition for our study has been carried out with a microprofilometer based on conoscopic holography [DGM*17, GMD17]. The spatial sampling of the original acquisitions was 0.025 mm for the silver coupons and, respectively, 0.05 mm for the bronze coupons.

Our study is aimed at verifying the possibility of characterizing modifications in the material roughness at a small scale using both standard roughness descriptors and other texture characterization methods used in the image processing domain. To test this idea, we processed depth maps cropping small patches (with real sizes 0.5 cm for both silver and bronze samples) and, after local background surface subtraction (planar surface), we independently estimated on each patch ISO roughness descriptors and texture features. The procedure has been repeated for uncoated and coated

samples at the different time steps.To ensure a fair comparison, we performed an accurate image registration using manually checked control points to align the depth images of the different time steps in the same reference grid.

The outcome of the procedure was, for each material, a set of depth texture patches labeled with a time step, as displayed in Figure 2. On these patches, we computed ISO areal roughness parameters and evaluated their capacity to distinguish between aging steps and we performed time classification experiments with ISO descriptors, classical image texture descriptors and CNN-based descriptors. Our pipeline, as presented in Figure 3 concludes with feeding the various descriptors into multiple classifiers and evaluating the accuracy of the aging classification for each of the studied materials.

3.1. ISO Roughness descriptors

We estimated ISO surface descriptors on patches using MountainsMap http://www.digitalsurf.com, a professional software tool widely applied in the surface metrology domain. Areal roughness parameter features from the ISO25178 standard [Bla13] are divided in groups (see Table 1) related to height statistics (e.g. S_q, root mean square height of the surface S_{sk}, S_{ku} skewness and kurtosis of height distribution), to spatial periodicity (e.g. S_{al} fastest decay auto-correlation rate, S_{tr}, texture aspect ratio of the surface, S_{td} texture direction of the surface), to the spatial shape of the data (S_{dq} root mean square gradient of the surface, S_{dr} developed area ratio), to the shape of the regions resulting from a watershed segmentation (S_{10z}, ten point height), to the features of the material ratio (Abbott-Firestone) bearing curve (S_{pk} reduced peak height, S_k core roughness depth, S_{mr1} upper bearing area, S_{mr2} lower bearing area). finally,

To understand which are the roughness descriptors most suitable to characterize material aging we used the approach proposed in [DKB14], e.g. we performed the analysis of variances (ANOVA). From the 3 groups of patches acquired at different time steps we estimated the F-score - the ratio between the variance of the means and the average of the sample variances for each group, which is an estimate of the overall population variance (assuming all groups have equal variances). Higher values of this score correspond to larger significance of the parameter variations across time steps.

3.2. Classical texture descriptors

The set of ISO descriptors is quite rich, but, actually does not include the most widely classical texture descriptors. There is a variety of 2D texture pattern characterization methods in the literature, and it is quite hard to tell which is the best for the characterization of a specific classes of patterns, as there are actually many different types of texture characterization with different invariance properties [LCF*18].

For fine-grained texture characterization, popular choices not included in the ISO sets are second order statistics, like gray co-occurrence matrix (COOM), specialized filter banks, e.g. MR8 [VZ03], local binary pattern (LBP) [OPM02].

Gray Level Co-occurrence Matrices sum the number of times

Table 1: *3D Roughness descriptors according to the ISO 25178 standard computed in this paper.*

3D Roughness descriptors defined by ISO 25178		
Height Parameters		
Sq	µm	Root-mean-square height
Ssk	-	Skewness
Sku	-	Kurtosis
Sp	µm	Maximum peak height
Sv	µm	Maximum pit height
Sz	µm	Maximum height
Sa	µm	Arithmetic mean height
Functional Parameters		
Smr	%	Areal material ratio
Smc	µm	Inverse areal material ratio
Sxp	µm	Extreme peak height
Spatial Parameters		
Sal	mm	Autocorrelation length
Str	-	Texture-aspect ratio
Std	°	Texture direction
Hybrid Parameters		
Sdq	-	Root-mean-square gradient
Sdr	%	Developed interfacial area ratio
Functional Parameters (Volume)		
Vm	mm^3/mm^2	Material volume
Vv	mm^3/mm^2	Void volume
Vmp	mm^3/mm^2	Peak material volume
Vmc	mm^3/mm^2	Core material volume
Vvc	mm^3/mm^2	Core void volume
Vvv	mm^3/mm^2	Pit void volume
Feature Parameters		
Spd	$1/mm^2$	Density of peaks
Spc	1/mm	Arithmetic mean peak curvature
S10z	µm	Ten point height
S5p	µm	Five point peak height
S5v	µm	Five point pit height
Sda	mm^2	Mean dale area
Sha	mm^2	Mean hill area
Sdv	mm^3	Mean dale volume
Shv	mm^3	Mean hill volume
Functional Parameters (Stratified surfaces)		
Sk	µm	Core roughness depth
Spk	µm	Reduced summit height
Svk	µm	Reduced valley depth
Smr1	%	Upper bearing area
Smr2	%	Lower bearing area

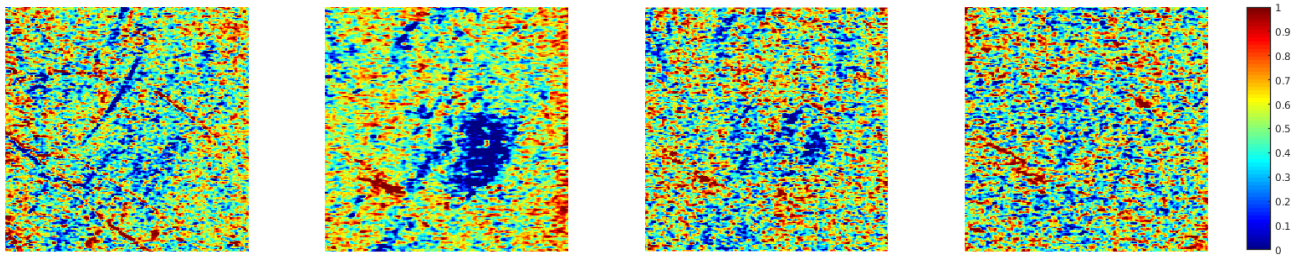

Figure 2: *Depth map patch from the uncoated silver sample, displayed at different aging labels (in order from left to right): t_0, t_1, t_2, t_3. The roughness changes from visible scratches at t_0 to the apparition of new high-depth elements at t_1 and finally, shifts to the formation of patina as it approaches t_3.*

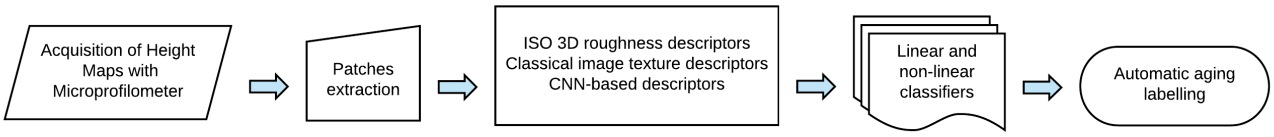

Figure 3: *Our workflow for aging classification of cultural heritage materials based on multiple roughness and texture descriptors.*

that a given pixel pair is found adjacent in the original gray-scale image. Based on this characterization of the spatial relationship between pixels, several statistics can be computed. In our application, we mapped the depth range of the whole set of patches within 32 gray levels, assuming isotropic texture and averaging x and y (horizontal and vertical) displacement vectors of length 1 and 3 pixels, estimating at the two scales contrast, correlation and energy features.These three features are estimated (contrast, correlation, energy), building a 6 component descriptor vector.

Local Binary Patterns encode the order relationship between a pixel and a given neighborhood. For each pixel, a binary array with a number of components equal to the size of the neighbourhood is computed, then histograms characterize the frequency of these values and are finally concatenated into a feature vector for the entire image. For our data, LBP features were extracted with rotational invariance [OPM02] with different values of radius (1,3) and circle sampling (8,16 points).

A simple and effective texture description may be obtained with the response of filter banks. The Maximum Response filter bank (MR8), described in [VZ02] characterizes patches with average and standard deviation of the maximal output of oriented filters as well as average and standard deviations of isotropically filtered values.

3.3. Texture descriptors based on pre-trained CNN

We evaluated state of the art CNN-based approaches by using features obtained from pre-trained deep networks as suggested in [CMK*14, CMKV16]. We tried different CNN-based texture labelling methods proposed in the cited papers: the penultimate fully connected layer of the pre-trained AlexNet architecture (FC-CNN) and, respectively, the convolutional layer from the pre-trained network VGG19, pooled into a Fisher vector (FV-CNN) representation. Due to the high dimensionality of the latter, amounting to an array size of 65k and computational limitations, the LDC and NEURC classifiers could not be tested for FV-CNN. Moreover, the number of patches per sample sums up to an average of approximately 100, which impeded a CNN fine-tuning approach.

3.4. Supervised labelling methods

Using the different kind of patch descriptors, we trained and tested different supervised classification methods. The classifiers cover different approaches including generative, discriminative, parametric and non parametric methods exploiting the implementations provided in the PRTools 5 Matlab package [dRTL*17] and in the LIBSVM library [CL11].

In our tests we compare a simple linear naive Bayesian classifier (ldc), linear support vector machine (libsvc), k-nearest neighbor (knnc), nonlinear Parzen classifier (parzenc) and non-linear feed-forward neural network with one hidden layer (neurc).

3.5. Patch classification tests

Using the extracted roughness descriptors on the patches' collections, we performed, for the different materials, a 10-fold cross-validation test to estimate accuracy in time label estimation with the different classifiers previously cited. In detail, we estimated the average classification error of 10 tests where we took 90% of the patches of each class as training set and the rest as test set. It is worth mentioning that for the classification based on the classical image texture descriptors and CNN features, data augmentation

(flip, rotation 90 degrees, rotation 180 degrees) was used to increase the collection of patches. On the contrary, since the ISO descriptors are rotation-invariant, there was no benefit in implementing data augmentation in this case.

3.6. Effects of coatings on age characterization

Another use of the microprofilometric measurements can be as well to evaluate how coatings influence the roughness. Coated surfaces have been captured and similarly characterized in small patches with ISO areal parameters and texture descriptors; differences with uncoated samples and evolution of parameters with time has been analyzed.

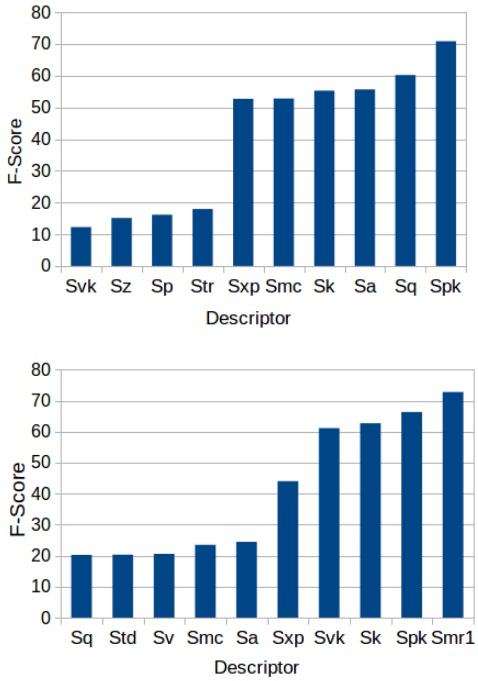

Figure 4: *Bar charts showing the ranking of the first 10 roughness descriptors based on the F-score (x-axis) computed with the ANOVA analysis. Top: Ranking for the uncoated silver sample. Bottom: Ranking for the uncoated bronze sample.*

4. Results

4.1. Best ISO descriptors for aging discrimination

To begin with, the analysis of ISO descriptors reveals that both type of surfaces have the most relevant roughness parameter (according to the F-score) belonging to the Functional parameters category recommended for stratifies surfaces, as can be noticed in 4. Hence, the changes for both uncoated silver and uncoated bronze seem to be reasonably quantified by the segmentation of local differences. Probably this is because the material bearing ratios characterize well stratified surfaces. Thus, the reduced peaks are the areas that are removed by initial abrasion in a surface and S_{pk} represents the average height of the reduced peaks. In addition, S_{mr1} describes the areal material ratio that divides the reduced peaks from the core surface, while S_{mr2} characterizes the areal material ratio that divides the reduced valleys from the core surface. To analyze the significance of the parameters to discriminate between different aging steps (t_0, t_1, t_2, t_3), we plotted the distribution of the most relevant descriptor for the uncoated silver and uncoated bronze samples, as well as for their coated variations, with box-and-whiskers plots in Figure 5. The medians of the patches corresponding to the three time steps are represented by the red line. These plots point out interesting behaviors.

First of all, as expected, on the uncoated silver samples, we measure significant differences for the most relevant roughness values at different times, that can actually be used to distinguish between the small patches at different time steps.

This is evident looking at the top left plot in Figure 5. Variations of S_{pk} are clearly statistically significant, especially comparing t_0 and t_1 (this is visible from the lack of overlap between the interquartile ranges represented by the blue rectangles). After t_1, differences are then less relevant with time, even if a decreasing trend is clear. Also the inter-sample variability of the roughness parameters is decreasing for the uncoated sample (see quartile boxes), suggesting that formation of patina tends to even the roughness and flatten the sample.

Looking at the evolution of the same parameter in the coated silver samples, however, it is possible to see that the behavior is not perpetuated and there are also large variations of the roughness descriptors. For C1 and C2, the medians seem to stay constant with aging as opposed to C3, where there is a dramatic change between t_0 and t_3, almost as in the case of the uncoated silver sample. This behavior suggests that, according to the S_{pk} ISO descriptor, C1 and C2 are more protective against aging than C3 for the silver material. The behavior of the variances is, however, quite strange, and this may be due to the irregular distribution of the coating creating local differences that may then differently evolve with aging.

The differences are less discernible in the case of bronze samples. Also in this case the most aging-discriminant feature (S_{mr1} changes significantly after the first time step for the uncoated sample, but then it seems constant. Differently from the silver, it appears quite difficult here to characterize age-related changes in roughness from ISO descriptors trends.

It can be therefore interesting to search for other possible texture descriptors that may characterize aging at a smaller scale. To investigate this, we compared several texture classification methods on the task of predicting correct time label from examples (extracted on the same sample).

4.2. Classification outcomes

Table 2 shows the classification accuracy obtained in the crossvalidation tests where we predict time labels of a subset of patches given the rest of the set as examples. As expected from the features behaviors previously described, all ISO descriptors provide quite poor results, even if it is possible to see that the accuracy is clearly higher on the uncoated materials, as expected. This should mean that the classification results are not due to over-fitting, but measure a real effect.

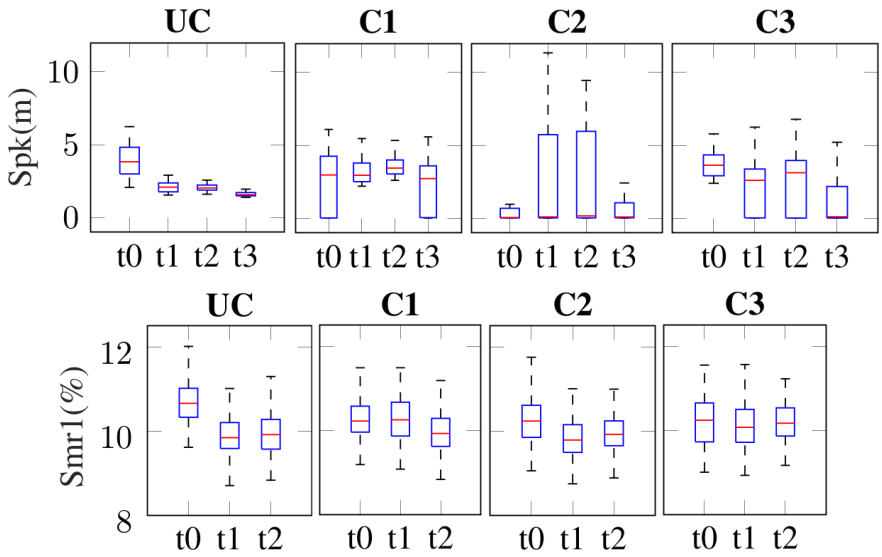

Figure 5: *Box plots showing the time evolution of the ISO feature with the highest F-score for time discrimination. Top: The S_{pk} feature for silver patches with different coatings: uncoated, one layer of acrylic, two layers of acrylic, one layer of acrylic + one layer of wax. Bottom: The S_{mr1} feature for the bronze patches with different coatings: uncoated, incral44, incral44 + wax, wax + incral44 + wax.*

			ISO	Image texture descriptors			CNN-based texture descriptors	
symbol	coating	classifier	all iso	coom	lbp	mr8	fv-cnn	fc-cnn
UC	uncoated 52 patches	LDC	0.53	0.34	0.18	**0.14**	-	0.75
		KNNC	0.38	0.37	0.41	0.25	0.18	**0.09**
		LIBSVC	0.39	0.49	0.39	0.13	0.13	**0.06**
		NEURC	0.42	0.19	**0.12**	0.16	-	0.59
		PARZENC	0.39	0.39	0.69	**0.23**	0.75	0.75
C1	1c acrylic 48 patches	LDC	0.66	0.49	**0.17**	0.32	-	0.75
		KNNC	0.55	0.51	0.43	0.46	0.37	**0.36**
		LIBSVC	0.71	0.61	0.51	0.35	**0.26**	0.31
		NEURC	0.60	0.40	**0.35**	0.37	-	0.62
		PARZENC	0.58	**0.51**	0.65	0.64	0.75	0.75
C2	2c acrylic 46 patches	LDC	0.75	0.59	**0.27**	0.51	-	0.75
		KNNC	0.73	0.55	0.60	**0.51**	0.46	0.58
		LIBSVC	0.67	0.61	0.59	0.57	**0.34**	0.47
		NEURC	0.76	**0.48**	0.51	0.60	-	0.67
		PARZENC	0.71	0.57	0.69	**0.56**	0.75	0.75
C3	1c acrylic + wax overlay 44 patches	LDC	0.62	0.67	**0.41**	**0.41**	-	0.75
		KNNC	0.59	0.51	0.52	0.49	**0.45**	**0.45**
		LIBSVC	0.64	0.65	0.55	0.42	0.34	**0.33**
		NEURC	0.59	0.56	0.55	**0.47**	-	0.70
		PARZENC	0.61	0.52	0.59	**0.51**	0.75	0.75

Table 2: *Error of cross-validated (10-folds) classifiers (from top to bottom: naive Bayes, k-nearest neighbour, support vector machine, neural network and parzen classifier) for aging prediction,performed on silver samples with different coatings and based on classical texture descriptors, neural net features and all the roughness parameters.*

			ISO	Image texture descriptors			CNN-based texture descriptors	
symbol	coating	classifier	all iso	coom	lbp	mr8	fv-cnn	fc-cnn
UC	uncoated 127 patches	LDC	0.47	**0.27**	0.33	0.29	-	0.67
		KNNC	0.48	0.36	0.53	0.46	**0.33**	0.38
		LIBSVC	0.49	0.41	0.39	0.29	**0.21**	0.32
		NEURC	0.52	0.33	0.35	**0.31**	-	0.60
		PARZENC	0.49	**0.40**	0.59	0.46	0.67	0.67
C1	incral44 116 patches	LDC	0.59	**0.51**	**0.51**	0.52	-	0.67
		KNNC	0.54	0.53	0.55	0.50	**0.48**	0.50
		LIBSVC	0.59	0.57	0.51	0.52	**0.39**	0.48
		NEURC	0.56	**0.48**	0.53	**0.48**	-	0.60
		PARZENC	0.58	0.55	0.66	**0.51**	0.67	0.67
C2	incral44 +wax 109 patches	LDC	0.60	0.31	**0.29**	0.33	-	0.67
		KNNC	0.60	0.43	0.55	0.45	**0.35**	0.36
		LIBSVC	0.59	0.52	0.37	0.32	**0.27**	0.28
		NEURC	0.55	0.35	**0.31**	0.35	-	0.53
		PARZENC	0.65	**0.45**	0.65	**0.45**	0.67	0.67
C3	wax + incral44 + wax 102 patches	LDC	0.46	0.43	**0.38**	0.41	-	0.67
		KNNC	0.48	0.58	0.51	0.52	**0.45**	0.49
		LIBSVC	0.45	0.66	0.43	0.40	**0.37**	0.43
		NEURC	0.44	0.41	0.40	**0.38**	-	0.57
		PARZENC	**0.46**	0.57	0.60	0.62	0.67	0.67

Table 3: *Error of cross-validated (10-folds) classifiers (from top to bottom: naive Bayes, k-nearest neighbour, support vector machine, neural network and parzen classifier) for aging prediction,performed on bronze samples with different coatings and based on classical texture descriptors, neural net features and all the roughness parameters.*

This behavior is maintained also by classifying with classical or CNN based texture descriptors. In this case, however, the classification of uncoated silver samples is quite accurate, with accuracy up to 94% using CNN based methods and close to 90% with local binary patterns (LBP). This means that it is possible to see that there are measurable effects of aging on high resolution texture.

For the bronze samples, we again have better results for the uncoated sample (see Table 3), meaning that there are measurable changes reduced by the use of coatings, even if the results are poorer.

It is clear that the results are not indicating a way to easily characterize the age of a surface with texture analysis, as each sample/artworks has different background texture due to the specific material treatment (brushing, polishing, etc.) that makes different objects not comparable.

But, for example, the classification outcomes provide interesting information about coatings' effects. The silver resulting in the highest overall classification error is C3 (one layer of acrylic plus one layer of wax), followed by C2 (two layers of acrylic) and lastly by C1 (one layer of acrylic). This suggests that for silver, the multi-layered coatings protect more than the single-layered coatings.

The magnitude of difference in surface variation with aging between variously coated samples is lower for the bronze dataset than it is for the silver dataset. Nonetheless, the most stable bronze coating over different aging steps is C1 (incral44), according to all descriptors. On the other hand, it seems that the coating C2 with a base layer of C1 (incrall44) and a top layer of wax has a higher aging discriminatory power. However, given the complex behaviour and interplay between the different protective films, it is difficult to assign the influence of each separate component in multi-coated cases.

5. Discussion

The analysis of the degradation of artworks' surfaces is a quite challenging task. In this paper we have shown that selected standard roughness descriptors used in material science, applied to surface geometry captured at a microscopic scale can reveal changes in the surface of metals across simulated aging steps. However, even if analyzed on a single metallic surface, only few roughness measurements seems to be uniform in the sample and to characterize the differences appearing in the artificial aging process. Furthermore, the amount of descriptors' changes decrease with time.

The differences in roughness seem to be better captured by classical or CNN based texture descriptors. This has been demonstrated with supervised labelling tests. The combinations of local texture descriptors and classifiers allow a reasonably successful classification of time steps given example patches from the same surface at the different time steps. This is not a pure overfitting effect, as it can be shown that, when a coating is applied on the metallic samples, the ability of the method to discriminate time steps is reduced or it disappears.

This means that the roughness analysis can be also exploited to assess the effects of different coatings used to reduce aging effects. Coatings actually makes aging differences in microgeometry less evident and are more stable with time variation.

The fact that texture analysis can capture aging related features suggests to further investigate the possibility of finding ways to

model aging effects with image processing applied to microprofilometry data. A possible idea could be to learn the association texture variations of patches with the related time interval.

Acknowledgements Work partially supported by the Scan4Reco project (EU Horizon 2020 Framework Programme for Research and Innovation, grant agreement no 665091), the DSURF project funded by the Italian Ministry of University and Research, and Sardinian Regional Authorities under projects VIGEC and Vis&VideoLab.

References

[Bla13] BLATEYRON F.: The areal field parameters. In *Characterisation of areal surface texture*. Springer, 2013, pp. 15–43. 1, 3

[Bun13] BUNGE H.-J.: *Texture analysis in materials science: mathematical methods*. Elsevier, 2013. 1

[CL11] CHANG C.-C., LIN C.-J.: LIBSVM: A library for support vector machines. *ACM Transactions on Intelligent Systems and Technology 2* (2011), 27:1–27:27. Software available at http:http://www.csie.ntu.edu.tw/~cjlin/libsvm. 4

[CMK*14] CIMPOI M., MAJI S., KOKKINOS I., MOHAMED S., VEDALDI A.: Describing textures in the wild. In *Proceedings of the IEEE Conference on Computer Vision and Pattern Recognition* (2014), pp. 3606–3613. 2, 4

[CMKV16] CIMPOI M., MAJI S., KOKKINOS I., VEDALDI A.: Deep filter banks for texture recognition, description, and segmentation. *International Journal of Computer Vision 118*, 1 (2016), 65–94. 2, 4

[DGM*17] DAFFARA C., GABURRO N., MARCHIORO G., ROMEO A., BASILISSI G., CAGNINI A., GALEOTTI M.: Surface microprofilometry for the assessment of the effects of traditional and innovative cleaning treatments of silver. In *Lasers in the Conservation of Artworks XI (Proceedings of International Conference LACONA XI)* (2017), Nicolaus Copernicus University Scientific Publishing House. doi:10.12775/3875-4.09. 2

[DKB14] DELTOMBE R., KUBIAK K., BIGERELLE M.: How to select the most relevant 3d roughness parameters of a surface. *Scanning 36*, 1 (2014), 150–160. 1, 3

[dRTL*17] DE RIDDER D., TAX D. M., LEI B., XU G., FENG M., ZOU Y., VAN DER HEIJDEN F.: Prtools introduction. *Classification, Parameter Estimation and State Estimation: An Engineering Approach Using MATLAB, 2nd Edition* (2017), 17–42. 4

[GMD17] GABURRO N., MARCHIORO G., DAFFARA C.: A versatile optical profilometer based on conoscopic holography sensors for acquisition of specular and diffusive surfaces in artworks. In *Optics for Arts, Architecture, and Archaeology VI* (2017), vol. 10331, International Society for Optics and Photonics, p. 103310A. 2

[GZZ10] GUO Z., ZHANG L., ZHANG D.: A completed modeling of local binary pattern operator for texture classification. *IEEE Transactions on Image Processing 19*, 6 (2010), 1657–1663. 1

[Har79] HARALICK R. M.: Statistical and structural approaches to texture. *Proceedings of the IEEE 67*, 5 (1979), 786–804. 1

[LCF*18] LIU L., CHEN J., FIEGUTH P., ZHAO G., CHELLAPPA R., PIETIKAINEN M.: A survey of recent advances in texture representation. *arXiv preprint arXiv:1801.10324* (2018). 3

[OPM02] OJALA T., PIETIKAINEN M., MAENPAA T.: Multiresolution gray-scale and rotation invariant texture classification with local binary patterns. *IEEE Transactions on pattern analysis and machine intelligence 24*, 7 (2002), 971–987. 3, 4

[RDS*15] RUSSAKOVSKY O., DENG J., SU H., KRAUSE J., SATHEESH S., MA S., HUANG Z., KARPATHY A., KHOSLA A., BERNSTEIN M., ET AL.: Imagenet large scale visual recognition challenge. *International Journal of Computer Vision 115*, 3 (2015), 211–252. 2

[SB00] STOUT K. J., BLUNT L.: *Three dimensional surface topography*. Elsevier, 2000. 1

[TJ*93] TUCERYAN M., JAIN A. K., ET AL.: Texture analysis. *Handbook of pattern recognition and computer vision 2* (1993), 235–276. 1

[VGBEM*10] VAN GORP A., BIGERELLE M., EL MANSORI M., GHIDOSSI P., IOST A.: Effects of working parameters on the surface roughness in belt grinding process: the size-scale estimation influence. *International Journal of Materials and Product Technology 38*, 1 (2010), 16–34. 1

[VZ02] VARMA M., ZISSERMAN A.: Classifying images of materials: Achieving viewpoint and illumination independence. *Computer VisionâĂŤECCV 2002* (2002), 255–271. 2, 4

[VZ03] VARMA M., ZISSERMAN A.: Texture classification: Are filter banks necessary? In *Computer vision and pattern recognition, 2003. Proceedings. 2003 IEEE computer society conference on* (2003), vol. 2, IEEE, pp. II–691. 2, 3